Available online at www.sciencedirect.com

ScienceDirect

Virology 367 (2007) 10–18

VIROLOGY

www.elsevier.com/locate/yviro

Effect of inhibition of dynein function and microtubule-altering drugs on AAV2 transduction

Sachiko Hirosue [a], Karin Senn [a], Nathalie Clément [a], Mathieu Nonnenmacher [a], Laure Gigout [a], R. Michael Linden [a,b], Thomas Weber [a,c,*]

[a] *Department of Gene and Cell Medicine, Mount Sinai School of Medicine, 1 Gustave L. Levy Place, Box 1496, New York, NY 10029-6514, USA*
[b] *Department of Microbiology, Mount Sinai School of Medicine, New York, NY 10029, USA*
[c] *Department of Molecular, Cell and Developmental Biology, Mount Sinai School of Medicine, New York, NY 10029, USA*

Received 4 January 2007; returned to author for revision 12 February 2007; accepted 2 May 2007
Available online 22 June 2007

Abstract

Over the past decade, adeno-associated (AAV) virus has emerged as an important vector for gene therapy. As a result, understanding its basic biology, including intracellular trafficking, has become increasingly important. Here, we describe the effect of inhibiting dynein function or altering the state of microtubule polymerization on rAAV2 transduction. Overexpression of dynamitin, resulting in a functional inhibition of the minus-end-directed microtubule motor protein dynein, did not inhibit transduction. Equally, treatment of cells with nocodazole, or concentrations of vinblastine that result in the disruption of microtubules, had no significant effect on transduction. In contrast, high concentrations of Taxol and vinblastine, resulting in microtubule stabilization and the formation of tubulin paracrystals respectively, reduced rAAV2 transduction in a vector-dose-dependent manner. These results demonstrate that AAV2 can infect HeLa cells independently of dynein function or an intact microtubule network.

Keywords: Adeno-associated virus; Microtubule; Dynamitin; Nocodazole; Vinblastine; Taxol; Trafficking

Introduction

Adeno-associated virus (AAV) is a small, non-enveloped, single-stranded DNA virus of the genus *Dependovirus* and the family Parvoviridae. As its name and classification indicate, AAV depends on a helper virus – which can be either adenovirus or herpes simplex virus – for a productive replication. In their absence, AAV can integrate its genome site specifically into the human chromosome 19 entering a so-called latent phase (Kotin et al., 1990; Samulski et al., 1991). Partly as a result of this unique trait as, well as its non-pathogenic nature, recombinant AAV has gained increasing attention as a gene therapy vector over the past decade (Wu et al., 2006). To develop fully the potential of AAV as a gene transfer vector, an understanding of its biology is crucial.

For successful transduction recombinant AAV2 (rAAV2) has to deliver its DNA to the nucleus. This process begins with the binding of rAAV2 to its primary receptor heparan sulfate proteoglycan (Summerford and Samulski, 1998) and one of several possible co-receptors (Asokan et al., 2006; Kashiwakura et al., 2005; Qing et al., 1999; Qiu and Brown, 1999; Qiu et al., 1999, 2000; Summerford et al., 1999). AAV2 is then endocytosed in a dynamin-dependent process (Bartlett et al., 2000; Duan et al., 1999). After endocytosis, AAV is transported to a perinuclear region. At present, it is unclear if this transport occurs while AAV2 is in the endosomal system or after its escape into the cytoplasm. From the perikaryon, the single-stranded DNA is then imported into the nucleus either as an intact viral particle (Hansen et al., 2001; Sonntag et al., 2006; Xiao et al., 2002) or after capsid disassembly (Lux et al., 2005). Despite considerable progress in recent years (reviewed in Ding et al., 2005), many aspects of the viral entry pathway of AAV remain to be elucidated in detail. In particular, the trafficking from the cell periphery to a perinuclear region remains incompletely understood.

* Corresponding author. Department of Gene and Cell Medicine, Mount Sinai School of Medicine, 1 Gustave L. Levy Place, Box 1496, New York, NY 10029-6514, USA. Fax: +1 212 849 2437.
E-mail address: thomas.weber@mssm.edu (T. Weber).

0042-6822/$ - see front matter © 2007 Elsevier Inc. All rights reserved.
doi:10.1016/j.virol.2007.05.009

Because of their size and the properties of the cytoplasm, it has been suggested that viruses and viral nucleocapsids cannot freely diffuse in the cytoplasm (Dohner and Sodeik, 2005; Luby-Phelps, 2000), although recent theoretical calculations have challenged this view for small viruses such as AAV (Dinh et al., 2005). Instead, several viruses such as adenovirus, herpes virus and rabies virus (Dohner and Sodeik, 2005) have been shown to take advantage of the minus-end-directed microtubule motor protein dynein to deliver their genomes to the perinuclear region.

Interestingly, it has been reported that a relative of AAV, canine parvovirus (CPV), also utilizes the dynein machinery for its transport to the perikaryon (Suikkanen et al., 2003; Vihinen-Ranta et al., 2000). Here we show that, in contrast to CPV, rAAV2 can transduce cells independently of dynein function and intact microtubules.

Results

Transport of cargo from the cell periphery towards the cell center often occurs along microtubules and is mediated by the minus-end-directed microtubule motor protein dynein. To analyze if transduction by rAAV2 is dependent on dynein function we overexpressed dynamitin in the cells to be infected. Dynamitin is a subunit of the dynactin complex and, if over-expressed, acts as a dominant-negative inhibitor of dynein function by disrupting the coupling of cargo and the dynein complex. Thus, overexpression of dynamitin has been used to demonstrate dynein mediated intracellular transport of adenovirus and herpes simplex virus 1 (Dohner et al., 2006; Suomalainen et al., 1999). To allow us to measure dynamitin expression, we generated an expression vector encoding for a fusion protein of dynamitin with the photostable red-fluorescent protein mCherry (Shaner et al., 2004). A plasmid encoding for mCherry alone served as a negative control.

In a first step, we confirmed the expression of functional levels of dynamitin by visualizing the *trans*-Golgi network protein p230 (Gleeson et al., 1996) in transfected cells 24 h post-transfection. As expected (Burkhardt, 1998), non-transfected cells and cells expressing mCherry displayed a classical perinuclear localization of the Golgi, while the Golgi was

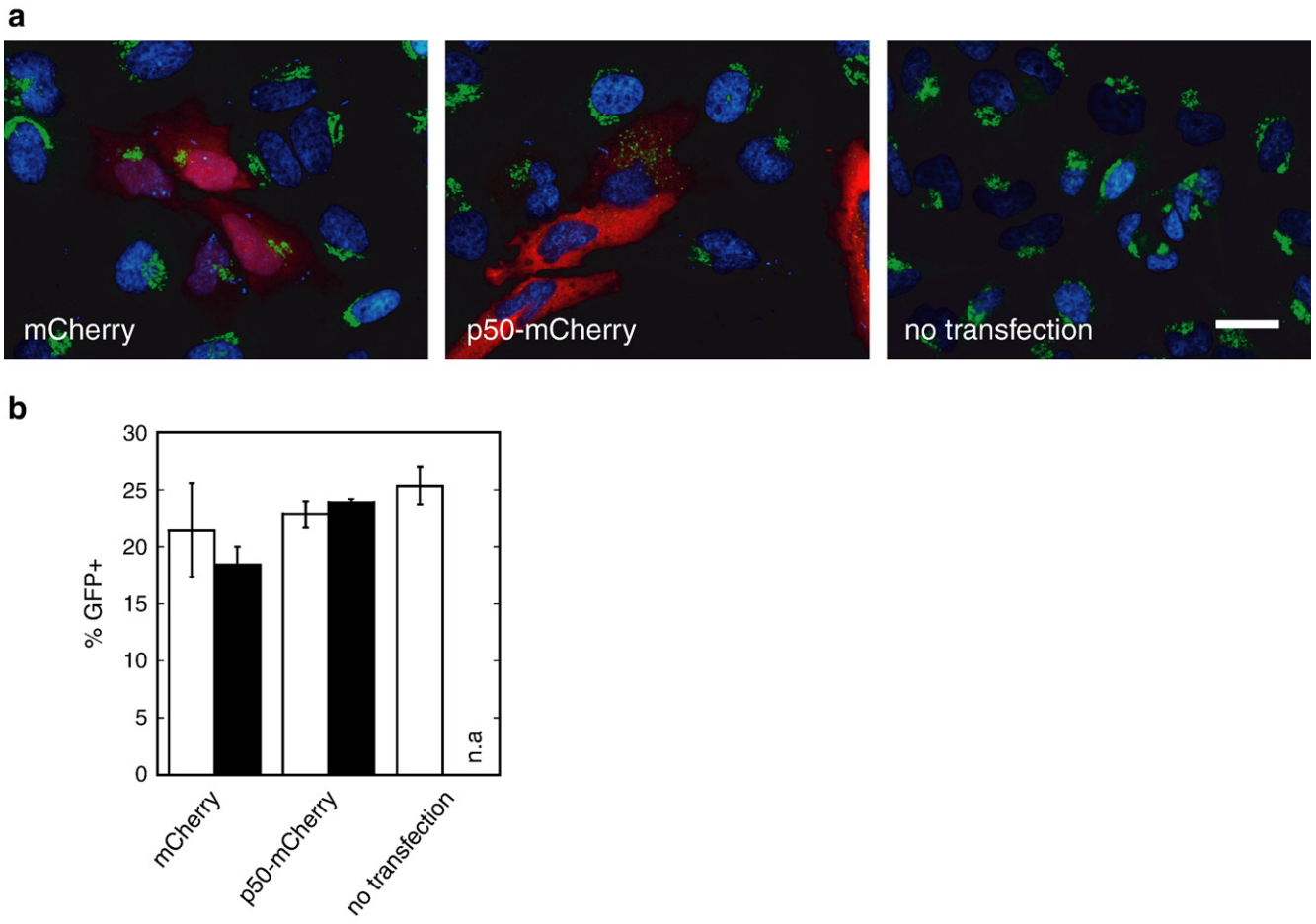

Fig. 1. Overexpression of dynamitin (p50) has no effect on rAAV2 transduction. (a) Effect of dynamitin overexpression on Golgi organization. HeLa cells were transfected with plasmids encoding mCherry (red) or dynamitin-mCherry (p50-mCherry, red). Twenty-four hours after transfection, the Golgi was visualized with an anti-p230 antibody (Alexa488, green), with the nucleus stained with DAPI (blue). Scale bar=25 μm. (b) Effect of dynamitin overexpression on rAAV2 transduction. Twenty-four hours after transfection with plasmids encoding mCherry or dynamitin-mCherry (p50-mCherry), HeLa cells were infected with rAAV2-GFP at 10^4 gcp/cell. Another 24 h later, cells gated for a coherent FSC/SSC population (10^4 cells in this population analyzed) were then analyzed for mCherry and GFP fluorescence by FACS. Open bars correspond to cells that were mCherry−, filled bars correspond to cells that were mCherry+. Transduction is shown as percent GFP-positive cells in each population. Error bars represent mean±SD (n=3).

dispersed throughout the cytoplasm in cells overexpressing dynamitin-mCherry (Fig. 1a).

We then proceeded to determine the effect of dynamitin overexpression on AAV transduction. Twenty-four hours after transfection of HeLa cells with either a plasmid encoding dynamitin-mCherry or a plasmid encoding mCherry alone, we added 10^4 genome containing particles (gcp) per cell of rAAV2 encoding GFP. Twenty-four hours after transduction, mCherry and GFP expression were analyzed by FACS. As can be seen from Fig. 1b, no difference in transduction could be detected between dynamitin-mCherry expressing and non-expressing cells. These results held true even for cells expressing the highest level of dynamitin-mCherry (data not shown). Similarly, overexpression of mCherry alone had no effect on transduction (Fig. 1b). Furthermore, non-transfected control samples were transduced to an equal extent. These data indicate that, at least in HeLa cells, dynein-mediated transport is not mandatory for a productive transduction with recombinant AAV2. This does not exclude, however, that dynein-dependent transduction pathways exist in addition.

An alternative way to determine whether transport along microtubules is important in viral trafficking is the alteration of the microtubule polymerization state with drugs such as nocodazole, vinblastine and Taxol.

Treatment of cells with nocodazole results in the disruption of microtubules (Jordan and Wilson, 1998). Previous studies analyzing the effect of nocodazole on rAAV2 transduction yielded conflicting results. One study reported an inhibition of rAAV2 transduction by nocodazole (Sanlioglu et al., 2000) while in a different study nocodazole had no effect (Alexander et al., 1994). In light of these discrepancies, we decided to study first the effect of nocodazole on rAAV2 transduction.

To this end, we pretreated HeLa cells for 4 h with various concentrations of nocodazole followed by infection with 10^4 gcp/cell rAAV2-GFP. After incubation for 24 h in the continued presence of the drug, we analyzed GFP expression by FACS analysis. As reported by Alexander and colleagues (1994), when using low concentrations of nocodazole, we observed no effect on AAV transduction. Conversely, as

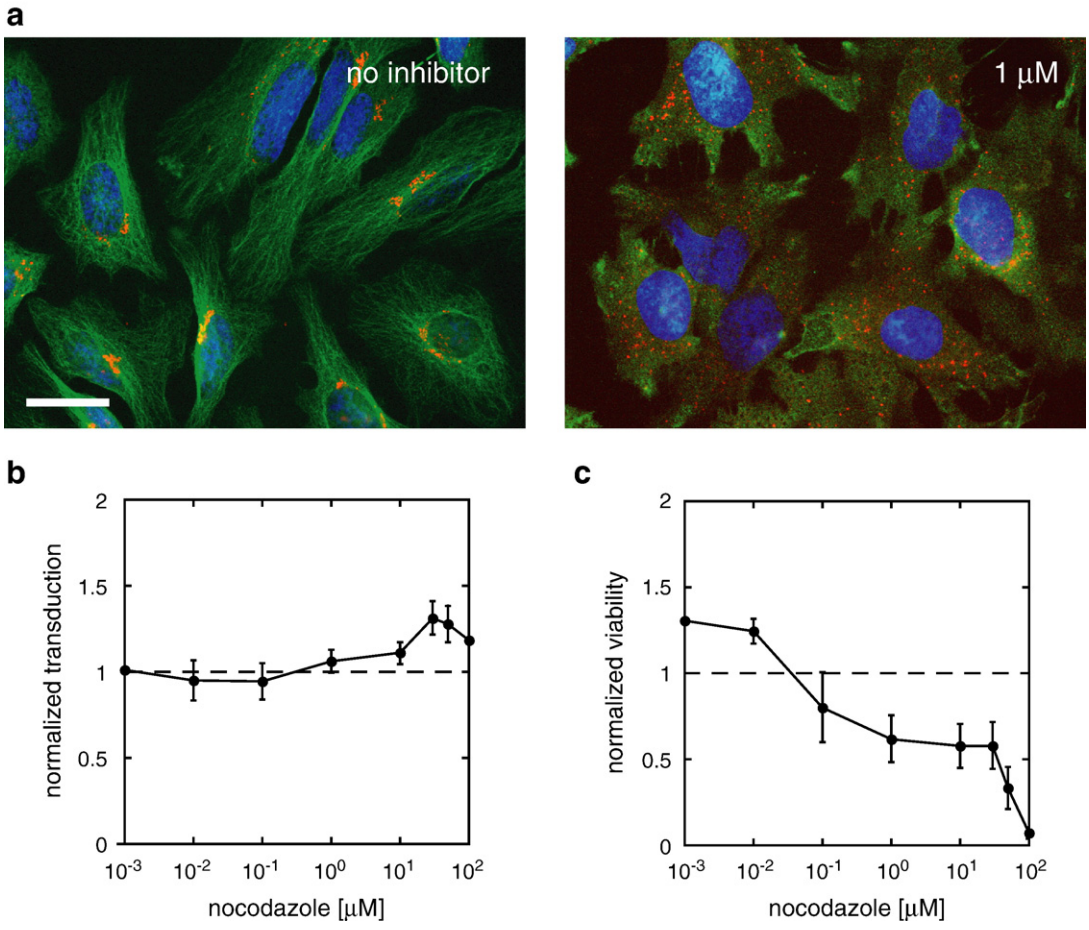

Fig. 2. Nocodazole does not inhibit rAAV2 transduction. (a) Microtubule and Golgi morphology. HeLa cells were preincubated in 1 μM nocodazole for 4 h and then fixed to observe the microtubule morphology (anti-beta-tubulin, Cy2, green) and Golgi localization (anti-p230, Cy3, red). Nuclei are in blue (DAPI). Scale bar=25 μm. (b) Percent GFP+ cells, normalized to no inhibitor control, as a function of nocodazole concentrations. After 4 h preincubation with the nocodazole concentrations indicated, HeLa cells were transduced with rAAV2-GFP at 10^4 gcp/cell. Twenty-four hours after transduction, the cells were harvested and stained with 7-amino-actinomycin D (7AAD) prior to FACS analysis for GFP. The GFP+ percentages were determined on the 7AAD-subset of a coherent population first defined by FSC/SSC. The %GFP populations were then normalized to a no inhibitor control represented by mean±SD. (c) Normalized viability as a function of nocodazole concentrations. Viability was defined as FSC/SSC coherent, 7AAD-population, which was then normalized to a no inhibitor control.

reported by others (Sanlioglu et al., 2000), we observed an inhibition of transduction at higher concentrations of the drug when we looked at the total population of cells (data not shown).

However, we also noticed that high concentrations of nocodazole were very toxic (Fig. 2c) and that – as a result of the drastic change in morphology caused by the disruption of microtubules – it is very challenging to determine the viability of nocodazole treated cells based on the forward/side scatter (FSC/SSC) profiles alone (Fig. S1a). Hence, we used an additional criterion for viability namely the exclusion of the live/dead cell dye 7-amino-actinomycin-D (7AAD). When we gated on cells that were alive – as determined by both their FSC/SSC profile and 7AAD exclusion (Fig. S1b) – no inhibition of AAV transduction by nocodazole, even at the highest concentration tested, was observed (Fig. 2b). Immunofluorescence microscopy revealed that in cells treated with nocodazole the microtubules were disrupted and the Golgi was, as expected (Burkhardt et al., 1997), dispersed throughout the cytoplasm (Fig. 2a).

Similar results were obtained with vinblastine, a drug that at low concentrations disrupts microtubules (Jordan and Wilson, 1998) and is less toxic than nocodazole (Fig. 3c). At concentrations of vinblastine that disrupt the microtubular network and disperse the Golgi (Fig. 3a, left), no effect on rAAV2 transduction could be observed (Fig. 3b). Interestingly, at higher concentrations of vinblastine, which result in the formation of tubulin paracrystals (Manfredi and Horwitz, 1984, and Fig. 3a, right), vinblastine partially inhibits transduction (Fig. 3b).

We next wanted to determine if Taxol, a drug known to stabilize microtubules (Jordan and Wilson, 1998), has any effect on AAV transduction. For this, we pretreated HeLa cells for 4 h with increasing concentrations of Taxol and analyzed GFP expression 24 h after addition of 10^4 gcp/cell rAAV-GFP. Fig. 4b shows that very high concentrations of Taxol were, in addition to being less toxic than nocodazole (Fig. 4c vs. Fig. 2c), able to inhibit partially AAV2 transduction—even if dead cells were rigorously excluded. At these concentrations, tubulin formed randomly initiated bundles at the end of which Golgi fragments are located (Fig. 4a and Wehland et al., 1983).

It has recently been reported that AAV trafficking is dependent on the vector dose used (Ding et al., 2006). To test if the role of microtubules in AAV2 transduction differs at

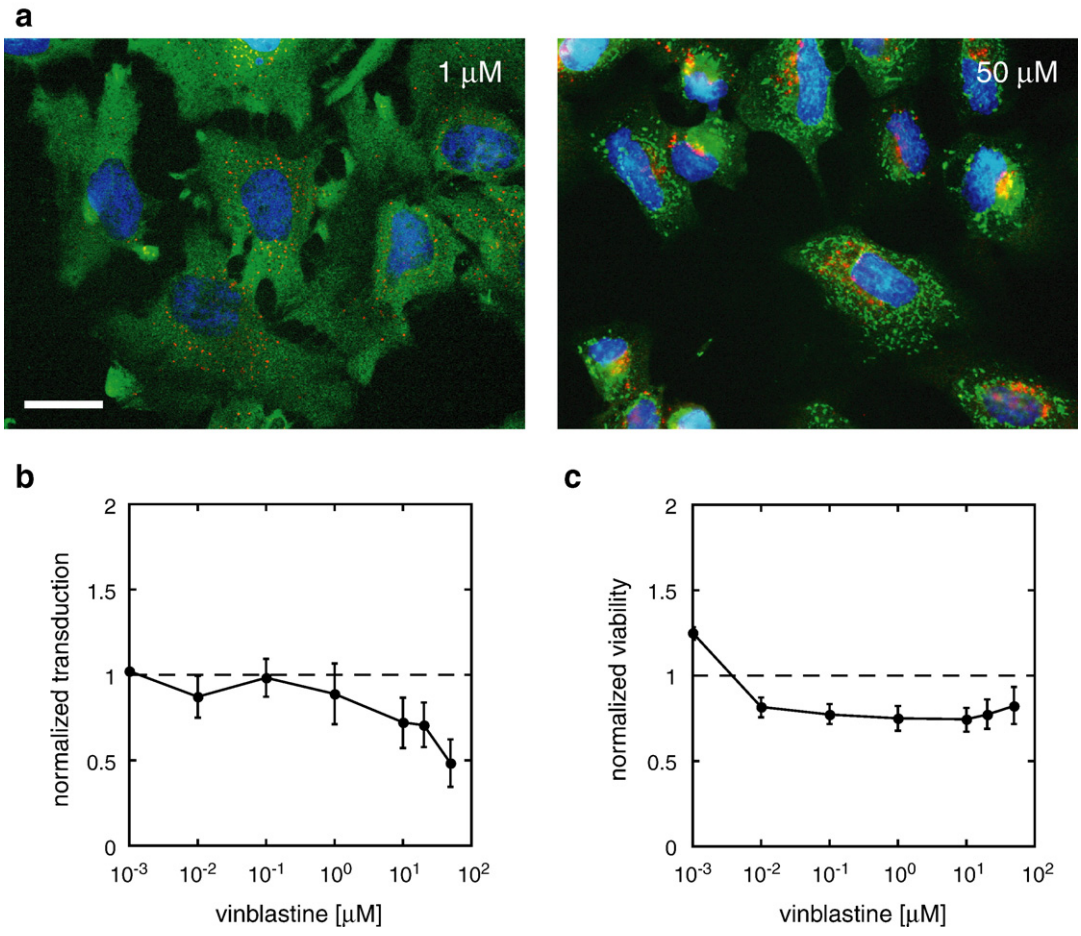

Fig. 3. Vinblastine has a concentration-dependent effect on rAAV2 transduction. Drug treatment and analysis was performed as in Fig. 2. (a) Microtubule and Golgi morphology. After 4 h preincubation with 1 μM (left) or 50 μM (right) vinblastine, microtubule morphology and Golgi distribution in HeLa cells were analyzed. Scale bar=25 μm. (b) Percent GFP+ cells, normalized to no inhibitor control, as a function of vinblastine concentrations. (c) Normalized viability as a function of vinblastine concentrations.

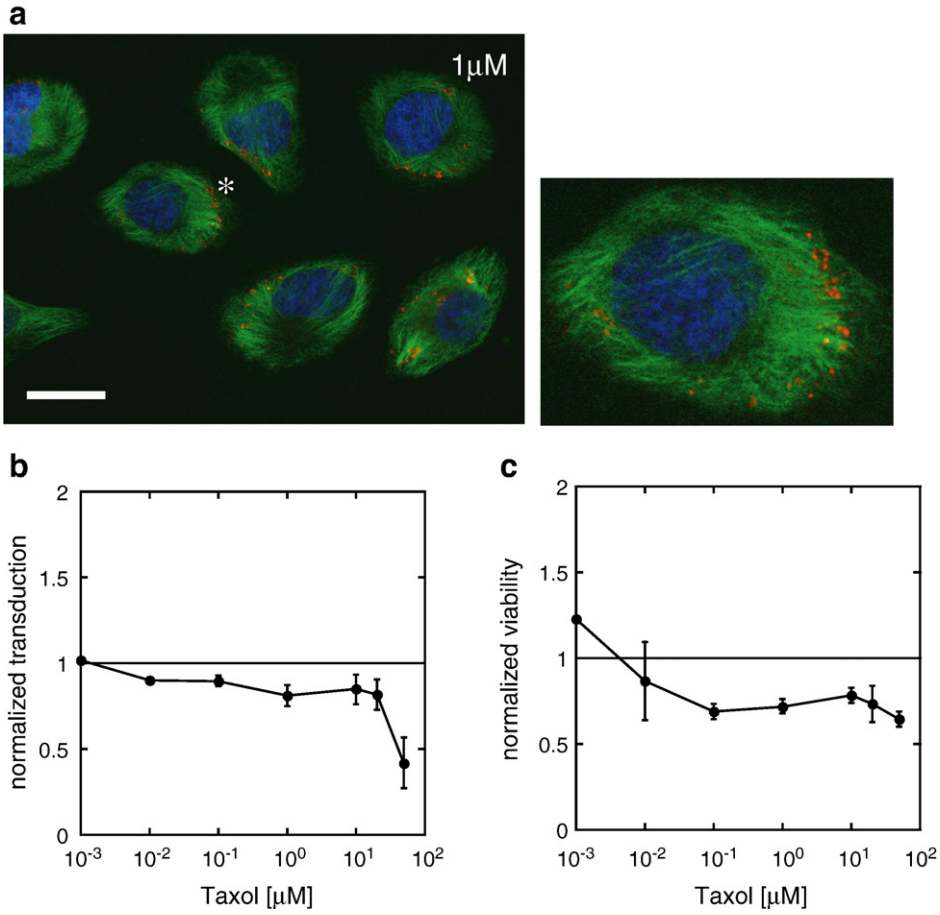

Fig. 4. High concentrations of Taxol partially inhibit rAAV2 transduction. Drug treatment and analysis was performed as in Fig. 2. (a) Microtubule and Golgi morphology. After 4 h incubation of HeLa cells with 1 μM Taxol, microtubule morphology and Golgi distribution in HeLa cells were analyzed. The cell noted with a white asterisk is enlarged to show the Golgi location with respect to the microtubules. Scale bar=25 μm. (b) Percent GFP+ cells, normalized to no inhibitor control, as a function of Taxol concentrations. (c) Normalized viability as a function of Taxol concentrations.

various viral particle to cell ratios, we analyzed the effect of microtubule-altering drugs at different vector doses. To allow us to use small viral particle to cell ratios in these experiments, we took advantage of self-complementary AAV2 preparations encoding for EGFP. Because transgene expression with these vectors is not dependent on double-strand synthesis, they display an earlier onset of transgene expression and transduce cells more readily (McCarty et al., 2001; Wang et al., 2003). As can be seen from Fig. 5, the effect of microtubule-altering drugs is, to a certain degree, dependent on vector dose. At a particle to cell ratio of 100, the inhibition of transduction by 50 μM Taxol (Fig. 5c, solid bars) or vinblastine (Fig. 5b, solid bars) was 60% and 69%, respectively. On the other hand, at a gcp/cell ratio of 1000 the relative reductions were approximately 45% and at a ratio of 10,000 only about 20% (Figs. 5c and b, solid bars). At a concentration of 1 μM, Taxol inhibited transduction as well and again more strongly at lower vector doses when compared to higher vector doses (Fig. 5c, open bars). As for single-stranded AAV (10^4 gcp/cell), high concentrations of nocodazole (50 μM) had no effect on AAV2 transduction (Fig. 5a, solid bars), regardless of the vector dose used. Low concentrations of nocodazole and vinblastine resulted in a slight inhibition of transduction (<20%) at the lowest vector dose (Figs. 5a and b, open bars). The significance – if any – of this potential inhibition is currently unknown. Importantly, however, we never observed any inhibition at high concentrations of nocodazole supporting the conclusion that complete disruption of microtubules does not affect AAV2 transduction. We also observed that the inhibition of transduction by high concentrations of Taxol and vinblastine at 10^4 gcp/cell was lower when we compare single-stranded and self-complementary virus (compare Figs. 2 and 5). The reason for this is likely that a smaller number of self-complementary vector particles is needed to result in a productive transduction because a potential rate-limiting step, i.e. double-strand synthesis, has been eliminated.

Together, our data show that neither dynein function nor an intact microtubule network is necessary for a productive transduction of HeLa cells by rAAV2. On the other hand, the partial inhibition of transduction by high concentrations of Taxol and vinblastine suggests that while intact microtubules are not required for transduction they might nevertheless play a complex role in rAAV2 transduction. Furthermore, the inhibitory effects of high concentrations of Taxol and vinblastine are vector dose dependent, the inhibition being most pronounced at low gcp/cell ratios. This behavior would be

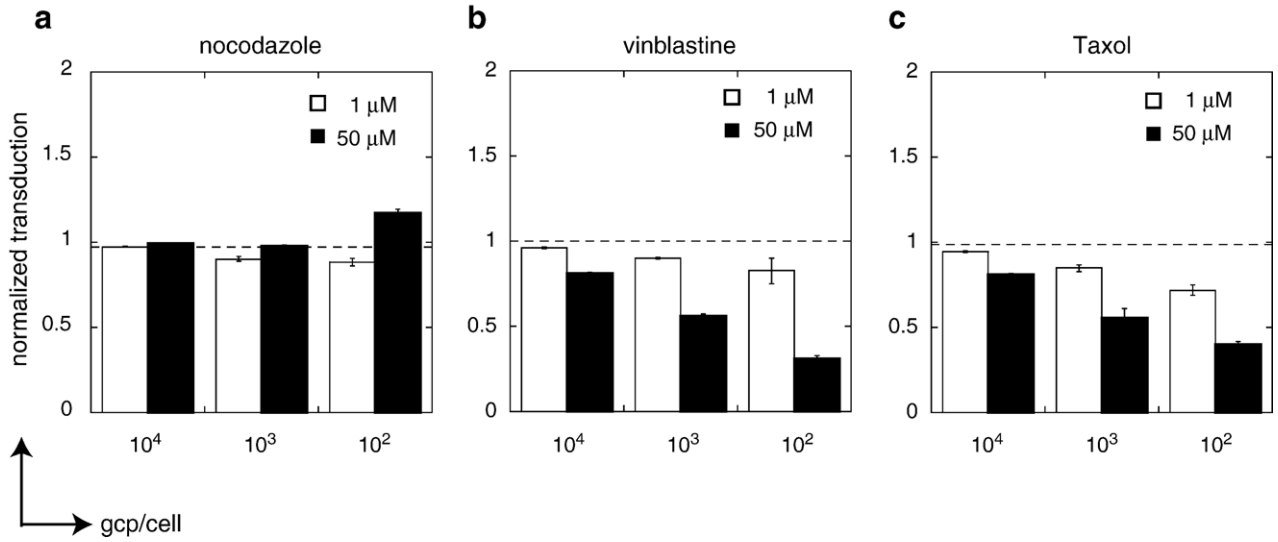

Fig. 5. Effect of microtubule-altering drugs on AAV2 transduction at various vector doses. Drug treatment and analysis were performed as in Fig. 2. (a) Percent GFP+ cells, normalized to no inhibitor control, as a function of nocodazole concentrations and vector dose. Open bars: 1 μM nocodazole; solid bars: 50 μM nocodazole. The vector dose indicated is in gcp/cell. (b) Percent GFP+ cells, normalized to no inhibitor control, as a function of vinblastine concentrations and vector dose. Open bars: 1 μM vinblastine; solid bars: 50 μM vinblastine. The vector dose indicated is in gcp/cell. (c) Percent GFP+ cells, normalized to no inhibitor control, as a function of Taxol concentrations and vector dose. Open bars: 1 μM Taxol; solid bars: 50 μM Taxol. The vector dose indicated is in gcp/cell.

consistent with a model of multiple productive pathways for AAV2 transduction.

Discussion

This study shows that, in contrast to many other viruses, recombinant AAV2 can transduce HeLa cells in a dynein and microtubule independent fashion. The cause for the lack of inhibition of recombinant AAV2 transduction by overexpression of dynamitin and the reason for the disparate results obtained when treating cells with nocodazole, vinblastine or Taxol, respectively, are currently unknown.

It is tempting to speculate, however, that the distinct effects that these treatments have on the cellular membrane system play a role in altering the level of AAV transduction. For instance, it has been shown that overexpression of dynamitin results in redistribution of lysosomes and late endosomes to the cell periphery (Burkhardt et al., 1997). Similarly, treatment of CV-1 cells with nocodazole, does not alter the perinuclear localization of lysosomes (Hamm-Alvarez et al., 1996), incubation with Taxol, on the other hand, disperses the lysosomes throughout the cytoplasm (Hamm-Alvarez et al., 1996). In addition to the endosomal system, other membrane bound compartments are affected by microtubule-altering drugs and inhibition of dynein function. For example, the localization of the Golgi is influenced as well (Burkhardt et al., 1997; Thyberg and Moskalewski, 1999, and Figs. 1–4a). This is of particular interest because it has been shown that both AAV2 (Pajusola et al., 2002) and AAV5 (Bantel-Schaal et al., 2002) can accumulate in the Golgi.

Because treatment of cells with microtubule-altering drugs drastically affects most endosomal membrane structures as well as the Golgi, it is not entirely surprising that immunofluorescence microscopy with the anti-capsid antibody A20 (Wobus et al., 2000) failed to show pronounced differences in virus distribution between untreated cells and cells treated with different concentrations of inhibitors (data not shown). An in depth analysis by both light and electron microscopy evaluating the co-localization of AAV with an array of subcellular markers will be needed to identify compartments in the endocytic system that contain AAV and are affected by microtubule-altering drugs. Because microscopic methods follow bulk virus, it will be paramount to confirm the involvement of specific compartments in transduction by functional assays, targeting distinct transport steps.

Recently, it has been reported that AAV2 can bind to the dynein machinery (Kelkar et al., 2006; Zhao et al., 2006). It appears therefore surprising that overexpression of dynamitin and disruption of microtubules with nocodazole or vinblastine does not result in inhibition of rAAV2 transduction. The simplest explanation for this apparent discrepancy is that both dynein-mediated as well as microtubule-independent pathways can result in productive rAAV2 transduction. Such dual modes of transport are not unprecedented. For instance, it has been shown that Shiga toxin can be transported to the nucleus by both microtubule dependent as well as independent mechanisms (Hehnly et al., 2006). Similarly, the transferrin receptor uses both microtubule dependent and independent recycling pathways (Lakadamyali et al., 2006). Furthermore, recent evidence that rAAV2 can traffic through either rab7 or rab11-positive endosomes (Ding et al., 2006) supports the notion that multiple infectious pathways exist for AAV2.

That the observed inhibition of rAAV2 transduction by high concentrations of vinblastine and Taxol are due to effects of these drugs on membrane bound organelles, such as endosomes or the Golgi, is only one possible explanation. It is also possible

that these drugs affect trafficking of rAAV2 after its escape into the cytoplasm. It has recently been shown that inclusion of a peptide into the AAV capsid that binds to the dynein light chain LC8 increases viral transduction (Xu et al., 2005). This suggests that, at least in certain cell types, transport of AAV to a perinuclear region, once it escaped into the cytoplasm, is a limiting step of transduction.

Clearly, much remains to be learned about the role of microtubules in AAV transduction. For instance, little is known on how AAV trafficking differs between cell types as well as AAV serotypes. Future studies, including light and electron microscopy and the use of functional assays that target specific transport modes, will be needed to shed light on the intricate role that microtubules play in AAV transduction. Understanding these trafficking patterns of AAV will play an important role in the development of future generations of AAV vectors for gene therapy.

Materials and methods

Materials

Nocodazole, Taxol (paclitaxel) and vinblastine sulfate were purchased from Sigma Aldrich (St. Louis, MO). Stock solutions were made at 20 mM in cell culture grade dimethylsulfoxide (DMSO) for nocodazole and Taxol, and in 50% (aq) ethanol for vinblastine.

Plasmid construction

The plasmid expressing the red-fluorescent protein mCherry (Shaner et al., 2004) under the control of a CMV promoter, was generated by replacing EGFP, in the vector pEGFP-N1 (Clontech), with mCherry. To this end, mCherry was amplified by PCR using the forward and reverse primers, 5′-GGTACCG-GAT CCTATGGTGA GCAAGGGCGA GGAGGATA-3′ and 5′-GCTTTAGCGG CCGCGTCACC TTACTTGTAC AGCTCGTCCA TGCCG-3′ and the plasmid pRSET-B-mCherry (Shaner et al., 2004) as the template. The PCR product was then cloned into the vector pEGFP-N1 digested with *Bam*HI and *Not*I. The plasmid encoding for a dynamitin (p50)-mCherry fusion protein was generated as described above except that EGFP was replaced in the vector p50-EGFP (Palazzo et al., 2001).

Cell culture and virus production

HeLa cells (ATCC, Manassas, VA) were maintained in MEM Eagle (Mediatech, Herndon, VA), 10% FBS (ATCC), 1:100 dilution of non-essential amino acids (Invitrogen, Carlsbad, CA) and sodium pyruvate (Invitrogen) at 37 °C and 5% CO unless otherwise noted.

Recombinant AAV was produced by the two-plasmid method (Grimm et al., 1998) and purified as described previously (Zhang et al., 2005). Particle and transducing titers were determined by real-time PCR using the method and primers described in (Gigout et al., 2005) or by real-time PCR using the primers CMV-F (5′-TCAATTACGGGGTCAT-TAGTT) and CMV-R (5′-ACTAATACGTAGATGTACTGCC).

Dynamitin experiments

HeLa cells were seeded at 4×10^4 cells/well in a 24-well plate in growth medium. Cells were transfected with Fugene 6 (Roche Diagnostics, Indianapolis, IN) according to the manufacturer using 3 μl Fugene 6 and 1 μg of plasmid DNA per 100 μl OptiMEM (Invitrogen). Forty microliters of the complexes were used per well. Twenty-four hours after transfection, the media was aspirated and rAAV2-GFP was added in fresh growth medium (10^4 gcp/cell). After an additional 24 h, dynamitin(p50)-mCherry and GFP expression were monitored on a FACScalibur (Becton-Dickinson, San Diego, CA). Tenthousand cells that were a coherent cluster on the forward and side scatter (FSC/SSC) were collected. The data were analyzed with Flojo (TreeStar, Ashland, OR). Live cells were gated based on the FSC/SSC profile. GFP and mCherry expression percentages were determined by quadrant analysis (GFP in FL1; mCherry in FL4) with the settings determined by appropriate single fluorophore controls.

In parallel, immunofluorescence microscopy was performed by seeding 1.7×10^4 cells into wells of 8-well Nunc Labtek II chamber slides. After overnight incubation, transfection was performed as described above except that only 10 μl of complexes per well were used. The slides were processed 24 h later for immunofluorescence microscopy as described below.

Microtubule inhibitor assay

HeLa cells were seeded at 4×10^4 cells/well in a 24-well plate in growth medium, incubated over night and pretreated for 4 h with different concentrations of inhibitors at constant solvent concentrations, 0.5% (v/v). The cells were then transduced with either single-stranded (10^4 gcp/cell) or self-complementary rAAV2 at vector doses ranging between 10^2 and 10^4 gcp/cell rAAV2. After incubation for 24 h in presence of the drug, cells were collected by trypsinization (including those cells in the supernatant and wash). GFP expression was analyzed by FACS as follows: after trypsinization, cells were resuspended in 100 μl 1× binding buffer with 5 μl (0.25 μg) of 7-amino-actinomycin D (7AAD, Annexin V-PE Apoptosis Detection Kit, BD Pharmingen, San Diego, CA). Cells were analyzed by FACS after 15 min at room temperature. Viable cells were defined by their FSC/SSC profiles and, in addition, their lack of 7AAD staining. GFP+ cells were determined by comparison with non-transfected control samples. In other words, to describe the above in order of gating, live cells were first determined in FSC/SSC as a coherent population. This population was then analyzed with FL1/FL4 and gated for FL4-negative cells. The GFP-positive cells are the percentage FL1 positive in this subset (see Fig. S1b). In parallel, immuno-fluorescence was performed by seeding 1.7×10^4 cells into wells of 8-well Nunc Labtek II chamber slides (Rochester, NY), treated with inhibitors for 4 h and prepared for immunofluor-escence microscopy as described below.

Immunofluorescence

After washing with PBS, cells were fixed with 4% paraformaldehyde in PBS for 20 min and permeabilized with 0.5% BSA, 0.02% saponin, 0.02% sodium azide in PBS (two-times 20 min). For experiments with p50-mCherry expression, the Golgi was localized with a monoclonal antibody directed against the *trans*-Golgi network protein p230 (BD Transduction Laboratories, Lexington, KY; 1:100 dilution, 1 h) and a goat-anti-mouse Alexa Fluor 488 IgG (H+L) (Invitrogen Molecular Probes, Portland, OR; 1:500 dilution, 30 min). Nuclei were visualized with DAPI (100 nM).

To analyze the effect of microtubule reorganization, microtubules were visualized with a polyclonal rabbit anti-beta-tubulin antibody (abcam, Cambridge, MA; 1:200 dilution, 1 h) and a secondary goat-anti-rabbit Cy2 antibody (Jackson ImmunoResearch, West Grove, PA; 1:200 dilution, 30 min). The Golgi was localized as described above except that a goat-anti-mouse Cy3 labeled secondary antibody (Jackson ImmunoResearch; 1:400 dilution 30 min) was used. Nuclei were stained with DAPI (100 nM). Slides were mounted using buffered gelvatol. All incubations were conducted at room temperature.

The slides were analyzed with a Leica DMRA2 (Leica Microsystems GmbH, Wetzler, Germany) fluorescence-microscope at 63-fold objective magnification and Hamamatsu ORCA-ER CCD camera (Opelco, Dulles, VA). Images were captured using Openlab 5.0.1 (Improvision, Lexington, MA) and deconvoluted using Volocity 3.6.1 (Improvision).

Acknowledgments

The authors would like to thank R. Vallee (Columbia University, New York, NY) for the kind gift of the plasmid p50-EGFP, X. Xiao (University of Pittsburgh, PA) for pds-AAV-CMV-GFP and R.Y. Tsien (University of California at San Diego, La Jolla, CA) for pRSET-B-mCherry. This work was supported by NIH grants GM073901, GM071023 to R.M.L. and GM066313, HL077322 to T.W.

Appendix A. Supplementary data

Supplementary data associated with this article can be found, in the online version, at doi:10.1016/j.virol.2007.05.009.

References

Alexander, I.E., Russell, D.W., Miller, A.D., 1994. DNA-damaging agents greatly increase the transduction of nondividing cells by adeno-associated virus vectors. J. Virol. 68 (12), 8282–8287.

Asokan, A., Hamra, J.B., Govindasamy, L., Agbandje-McKenna, M., Samulski, R.J., 2006. Adeno-associated virus type 2 contains an integrin alpha5beta1 binding domain essential for viral cell entry. J. Virol. 80 (18), 8961–8969.

Bantel-Schaal, U., Hub, B., Kartenbeck, J., 2002. Endocytosis of adeno-associated virus type 5 leads to accumulation of virus particles in the Golgi compartment. J. Virol. 76 (5), 2340–2349.

Bartlett, J.S., Wilcher, R., Samulski, R.J., 2000. Infectious entry pathway of adeno-associated virus and adeno-associated virus vectors. J. Virol. 74 (6), 2777–2785.

Burkhardt, J.K., 1998. The role of microtubule-based motor proteins in maintaining the structure and function of the Golgi complex. Biochim. Biophys. Acta 1404 (1–2), 113–126.

Burkhardt, J.K., Echeverri, C.J., Nilsson, T., Vallee, R.B., 1997. Overexpression of the dynamitin (p50) subunit of the dynactin complex disrupts dynein-dependent maintenance of membrane organelle distribution. J. Cell Biol. 139 (2), 469–484.

Ding, W., Zhang, L., Yan, Z., Engelhardt, J.F., 2005. Intracellular trafficking of adeno-associated viral vectors. Gene Ther. 12 (11), 873–880.

Ding, W., Zhang, L.N., Yeaman, C., Engelhardt, J.F., 2006. rAAV2 traffics through both the late and the recycling endosomes in a dose-dependent fashion. Mol. Ther. 13 (4), 671–682.

Dinh, A.T., Theofanous, T., Mitragotri, S., 2005. A model for intracellular trafficking of adenoviral vectors. Biophys. J. 89 (3), 1574–1588.

Dohner, K., Sodeik, B., 2005. The role of the cytoskeleton during viral infection. Curr. Top. Microbiol. Immunol. 285, 67–108.

Dohner, K., Radtke, K., Schmidt, S., Sodeik, B., 2006. Eclipse phase of herpes simplex virus type 1 infection: efficient dynein-mediated capsid transport without the small capsid protein VP26. J. Virol. 80 (16), 8211–8224.

Duan, D., Li, Q., Kao, A.W., Yue, Y., Pessin, J.E., Engelhardt, J.F., 1999. Dynamin is required for recombinant adeno-associated virus type 2 infection. J. Virol. 73 (12), 10371–10376.

Gigout, L., Rebollo, P., Clement, N., Warrington Jr., K.H., Muzyczka, N., Linden, R.M., Weber, T., 2005. Altering AAV tropism with mosaic viral capsids. Mol. Ther. 11 (6), 856–865.

Gleeson, P.A., Anderson, T.J., Stow, J.L., Griffiths, G., Toh, B.H., Matheson, F., 1996. p230 is associated with vesicles budding from the *trans*-Golgi network. J. Cell Sci. 109 (Pt. 12), 2811–2821.

Grimm, D., Kern, A., Rittner, K., Kleinschmidt, J.A., 1998. Novel tools for production and purification of recombinant adenoassociated virus vectors. Hum. Gene Ther. 9 (18), 2745–2760.

Hamm-Alvarez, S.F., Sonee, M., Loran-Goss, K., Shen, W.C., 1996. Paclitaxel and nocodazole differentially alter endocytosis in cultured cells. Pharm. Res. 13 (11), 1647–1656.

Hansen, J., Qing, K., Srivastava, A., 2001. Infection of purified nuclei by adeno-associated virus 2. Mol. Ther. 4 (4), 289–296.

Hehnly, H., Sheff, D., Stamnes, M., 2006. Shiga toxin facilitates its retrograde transport by modifying microtubule dynamics. Mol. Biol. Cell 17 (10), 4379–4389.

Jordan, M.A., Wilson, L., 1998. Use of drugs to study role of microtubule assembly dynamics in living cells. Methods Enzymol. 298, 252–276.

Kashiwakura, Y., Tamayose, K., Iwabuchi, K., Hirai, Y., Shimada, T., Matsumoto, K., Nakamura, T., Watanabe, M., Oshimi, K., Daida, H., 2005. Hepatocyte growth factor receptor is a coreceptor for adeno-associated virus type 2 infection. J. Virol. 79 (1), 609–614.

Kelkar, S., De, B.P., Gao, G., Wilson, J.M., Crystal, R.G., Leopold, P.L., 2006. A common mechanism for cytoplasmic dynein-dependent microtubule binding shared among adeno-associated virus and adenovirus serotypes. J. Virol. 80 (15), 7781–7785.

Kotin, R.M., Siniscalco, M., Samulski, R.J., Zhu, X.D., Hunter, L., Laughlin, C.A., McLaughlin, S., Muzyczka, N., Rocchi, M., Berns, K.I., 1990. Site-specific integration by adeno-associated virus. Proc. Natl. Acad. Sci. U. S. A. 87 (6), 2211–2215.

Lakadamyali, M., Rust, M.J., Zhuang, X., 2006. Ligands for clathrin-mediated endocytosis are differentially sorted into distinct populations of early endosomes. Cell 124 (5), 997–1009.

Luby-Phelps, K., 2000. Cytoarchitecture and physical properties of cytoplasm: volume, viscosity, diffusion, intracellular surface area. Int. Rev. Cytol. 192, 189–221.

Lux, K., Goerlitz, N., Schlemminger, S., Perabo, L., Goldnau, D., Endell, J., Leike, K., Kofler, D.M., Finke, S., Hallek, M., Buning, H., 2005. Green fluorescent protein-tagged adeno-associated virus particles allow the study of cytosolic and nuclear trafficking. J. Virol. 79 (18), 11776–11787.

Manfredi, J.J., Horwitz, S.B., 1984. Vinblastine paracrystals from cultured cells are calcium-stable. Exp. Cell Res. 150 (1), 205–212.

McCarty, D.M., Monahan, P.E., Samulski, R.J., 2001. Self-complementary recombinant adeno-associated virus (scAAV) vectors promote efficient

transduction independently of DNA synthesis. Gene Ther. 8 (16), 1248–1254.
Pajusola, K., Gruchala, M., Joch, H., Luscher, T.F., Yla-Herttuala, S., Bueler, H., 2002. Cell-type-specific characteristics modulate the transduction efficiency of adeno-associated virus type 2 and restrain infection of endothelial cells. J. Virol. 76 (22), 11530–11540.
Palazzo, A.F., Joseph, H.L., Chen, Y.J., Dujardin, D.L., Alberts, A.S., Pfister, K.K., Vallee, R.B., Gundersen, G.G., 2001. Cdc42, dynein, and dynactin regulate MTOC reorientation independent of Rho-regulated microtubule stabilization. Curr. Biol. 11 (19), 1536–1541.
Qing, K., Mah, C., Hansen, J., Zhou, S., Dwarki, V., Srivastava, A., 1999. Human fibroblast growth factor receptor 1 is a co-receptor for infection by adeno-associated virus 2. Nat. Med. 5 (1), 71–77.
Qiu, J., Brown, K.E., 1999. Integrin alphaVbeta5 is not involved in adeno-associated virus type 2 (AAV2) infection. Virology 264 (2), 436–440.
Qiu, J., Mizukami, H., Brown, K.E., 1999. Adeno-associated virus 2 co-receptors? Nat. Med. 5 (5), 467–468.
Qiu, J., Handa, A., Kirby, M., Brown, K.E., 2000. The interaction of heparin sulfate and adeno-associated virus 2. Virology 269 (1), 137–147.
Samulski, R.J., Zhu, X., Xiao, X., Brook, J.D., Housman, D.E., Epstein, N., Hunter, L.A., 1991. Targeted integration of adeno-associated virus (AAV) into human chromosome 19. EMBO J. 10 (12), 3941–3950.
Sanlioglu, S., Benson, P.K., Yang, J., Atkinson, E.M., Reynolds, T., Engelhardt, J.F., 2000. Endocytosis and nuclear trafficking of adeno-associated virus type 2 are controlled by rac1 and phosphatidylinositol-3 kinase activation. J. Virol. 74 (19), 9184–9196.
Shaner, N.C., Campbell, R.E., Steinbach, P.A., Giepmans, B.N., Palmer, A.E., Tsien, R.Y., 2004. Improved monomeric red, orange and yellow fluorescent proteins derived from Discosoma sp. red fluorescent protein. Nat. Biotechnol. 22 (12), 1567–1572.
Sonntag, F., Bleker, S., Leuchs, B., Fischer, R., Kleinschmidt, J.A., 2006. Adeno-associated virus type 2 capsids with externalized VP1/VP2 trafficking domains are generated prior to passage through the cytoplasm and are maintained until uncoating occurs in the nucleus. J. Virol. 80 (22), 11040–11054.
Suikkanen, S., Aaltonen, T., Nevalainen, M., Valilehto, O., Lindholm, L., Vuento, M., Vihinen-Ranta, M., 2003. Exploitation of microtubule cytoskeleton and dynein during parvoviral traffic toward the nucleus. J. Virol. 77 (19), 10270–10279.
Summerford, C., Samulski, R.J., 1998. Membrane-associated heparan sulfate proteoglycan is a receptor for adeno-associated virus type 2 virions. J. Virol. 72 (2), 1438–1445.
Summerford, C., Bartlett, J.S., Samulski, R.J., 1999. AlphaVbeta5 integrin: a co-receptor for adeno-associated virus type 2 infection. Nat. Med. 5 (1), 78–82.
Suomalainen, M., Nakano, M.Y., Keller, S., Boucke, K., Stidwill, R.P., Greber, U.F., 1999. Microtubule-dependent plus-and minus end-directed motilities are competing processes for nuclear targeting of adenovirus. J. Cell Biol. 144 (4), 657–672.
Thyberg, J., Moskalewski, S., 1999. Role of microtubules in the organization of the Golgi complex. Exp. Cell Res. 246 (2), 263–279.
Vihinen-Ranta, M., Yuan, W., Parrish, C.R., 2000. Cytoplasmic trafficking of the canine parvovirus capsid and its role in infection and nuclear transport. J. Virol. 74 (10), 4853–4859.
Wang, Z., Ma, H.I., Li, J., Sun, L., Zhang, J., Xiao, X., 2003. Rapid and highly efficient transduction by double-stranded adeno-associated virus vectors in vitro and in vivo. Gene Ther. 10 (26), 2105–2111.
Wehland, J., Henkart, M., Klausner, R., Sandoval, I.V., 1983. Role of microtubules in the distribution of the Golgi apparatus: effect of Taxol and microinjected anti-alpha-tubulin antibodies. Proc. Natl. Acad. Sci. U. S. A. 80 (14), 4286–4290.
Wobus, C.E., Hugle-Dorr, B., Girod, A., Petersen, G., Hallek, M., Kleinschmidt, J.A., 2000. Monoclonal antibodies against the adeno-associated virus type 2 (AAV-2) capsid: epitope mapping and identification of capsid domains involved in AAV-2-cell interaction and neutralization of AAV-2 infection. J. Virol. 74 (19), 9281–9293.
Wu, Z., Asokan, A., Samulski, R.J., 2006. Adeno-associated virus serotypes: vector toolkit for human gene therapy. Mol. Ther. 14 (3), 316–327.
Xiao, W., Warrington Jr., K.H., Hearing, P., Hughes, J., Muzyczka, N., 2002. Adenovirus-facilitated nuclear translocation of adeno-associated virus type 2. J. Virol. 76 (22), 11505–11517.
Xu, J., Ma, C., Bass, C., Terwilliger, E.F., 2005. A combination of mutations enhances the neurotropism of AAV-2. Virology 341 (2), 203–214.
Zhang, N., Clement, N., Chen, D., Fu, S., Zhang, H., Rebollo, P., Linden, R.M., Bromberg, J.S., 2005. Transduction of pancreatic islets with pseudotyped adeno-associated virus: effect of viral capsid and genome conversion. Transplantation 80 (5), 683–690.
Zhao, W., Zhong, L., Wu, J., Chen, L., Qing, K., Weigel-Kelley, K.A., Larsen, S. H., Shou, W., Warrington Jr., K.H., Srivastava, A., 2006. Role of cellular FKBP52 protein in intracellular trafficking of recombinant adeno-associated virus 2 vectors. Virology 353 (2), 283–293.